

Transverse Spectra in High-Energy Nucleus-Nucleus Collisions

Fu-Hu Liu^y

*Institute of Modern Physics and Department of Physics, Shanxi Teachers University,
Linfen, Shanxi 041004, China*

(Received October 17, 2000)

The transverse momentum and transverse mass distributions of negative hadrons and protons produced in high-energy nucleus-nucleus collisions are studied by a multisource ideal gas model. The calculated results are compared and found to be in good agreement with the NA49 experimental data of central Pb-Pb collisions at 158A GeV.

PACS. 25.75.-q – Relativistic heavy-ion collisions.

PACS. 25.75.Dw – Particle and resonance production.

PACS. 24.10.Pa – Thermal and statistical models.

I. Introduction

The aim of high-energy nucleus-nucleus collisions, especially at the Brookhaven Alternating Gradient Synchrotron (AGS) and the CERN Super Proton Synchrotron (SPS), is to investigate nuclear matter under extreme conditions, i.e., high temperature and high density [1]. The thermal character of such interacting systems is an exciting prospect. Rapidity distributions of produced particles in high-energy nucleus-nucleus collisions reflect the longitudinal motion of the interacting system, while transverse momentum and transverse mass distributions reflect a transverse excitation of the interacting system. In the rest frame of the emission source of the produced particles, the transverse excitation degree of the interacting system is in fact the excitation degree of the emission source.

Several dynamical microscopic models [2-13] have been used to describe high-energy nucleus-nucleus collisions. Most of them describe the early prehadronic phase and hadronization in terms of the string picture for the high-energy hadronic interactions [2-10]. Some of them are based on the concept that the colliding nuclei can be decomposed into their parton substructure [11-13].

In contrast to microscopic models, thermal models have been employed due to their simplicity [14-17]. Here the hot and dense system is assumed to be in local thermal and chemical equilibrium at the time of freeze-out. Thermal models state nothing about the history of the fireball, whether it was created by a pure hadronic system or a quark-gluon plasma. Nevertheless, thermal models are attractive, because they predict all of the particle abundances in terms of only three parameters, the temperature (or the momentum distribution width), the baryochemical potential and the volume of the fireball.

The simplest thermal model is Maxwell's ideal gas model which can be found in any textbook of classical physics. Based on the ideal gas model, we can explain some experimental results of high-energy nucleus-nucleus collisions. For example, the emission angular distribution

of light nuclear fragments [18] and the pseudorapidity (angular) distribution of relativistic particles [19-21] can be explained in fact by a multisource ideal gas model. That is to say that we can treat the two-source emission picture for light nuclear fragments [18] and the thermalized cylinder model for relativistic particles [19-21] as a result of the multisource ideal gas model.

In this paper, we use the multisource ideal gas model to describe the transverse momentum and transverse mass distributions of negative hadrons and protons produced in central Pb-Pb collisions at 158A GeV. The calculated results are compared with the experimental data of the NA49 Collaboration [22].

II. The model

It is expected that a thermalized cylinder is formed in high-energy nucleus-nucleus collisions along the incoming direction of the projectile [19-21]. Many emission sources exist in the thermalized cylinder. In the laboratory reference frame, the rapidities of the two endpoints of the thermalized cylinder are y_{\min} and y_{\max} . The emission sources stay at different rapidities in the range from y_{\min} to y_{\max} [19-21]. As in the ideal gas model, in the rest frame of the emission source i , we assume that the three components of particle momentum obey a Gaussian distribution and have the same standard deviation (distribution width) \mathcal{M}_i . According to our discussion, the different emission sources have different rapidities and may stay in different excitation degrees.

The transverse momentum P_T obeys the Rayleigh distribution

$$f_{P_T}(P_T; \mathcal{M}_i) = \frac{P_T}{\mathcal{M}_i^2} \exp\left[-\frac{P_T^2}{2\mathcal{M}_i^2}\right] \quad (1)$$

It is a normalized distribution. We may select different rapidity windows to study the P_T distribution of the produced particles. For a given rapidity window, the particles are contributed by many emission sources with different probabilities.

In the rapidity window $y = y_a$ to y_b , if the first emission source contributes A_1 , the second emission source contributes A_2 , ..., and the last emission source contributes A_n , then the final P_T distribution can be written as

$$f_{P_T}(P_T) = \sum_{i=1}^n A_i f_{P_T}(P_T; \mathcal{M}_i) \quad (2)$$

where \mathcal{M}_i is the P_T distribution width corresponding to the i th emission source. A simple Monte Carlo calculation can give the P_T distribution for a given rapidity window in the case of different \mathcal{M}_i [21]. However, Eq. (1) can describe directly the P_T distribution for a given rapidity window in the case of the same \mathcal{M}_i . For the later case, the same \mathcal{M}_i is in fact the P_T distribution width of particles in a given rapidity window.

The distribution of transverse mass ($m_T = \sqrt{P_T^2 + m_0^2}$) of particles produced in the emission source i is given by

$$f_{m_T}(m_T; \mathcal{M}_i) = \frac{m_T}{\mathcal{M}_i^2} \exp\left[-\frac{m_T^2 - m_0^2}{2\mathcal{M}_i^2}\right] \quad (3)$$

where m_0 is the rest mass of a produced particle. The final m_T distribution, contributed by all n emission sources, is

$$f_{m_T}(m_T) = \prod_{i=1}^n A_i f_{m_T}(m_T; \gamma_i); \quad (4)$$

Let y_i denote the rapidity of emission source i in the laboratory reference frame. In the case of different γ_i , the relationship between γ_i and y_i is not easily determined. If we regard the γ_i as free parameters, then there are too many free parameters introduced in the model. For the purpose of convenience, we divide the thermalized cylinder into three parts. The excitation degrees of emission sources staying in the same part are regarded as the same.

Generally speaking, the central region around midrapidity $y_c = (y_{\min} + y_{\max})/2$ in the thermalized cylinder stays at a high excitation state. The regions around the two endpoints in the thermalized cylinder stay at a low excitation state. While the residual regions stay at a middle excitation state. If the rapidity shift of projectile or target nucleus with respect to the midrapidity is $3\pm y$, then $\pm y = (y_{\max} - y_{\min})/6$: The first part with high excitation degree stays in the rapidity range from $y_c - \pm y$ to $y_c + \pm y$. The second part with middle excitation degree stays in the rapidity regions from $y_{\min} + \pm y$ to $y_c - \pm y$ and $y_c + \pm y$ to $y_{\max} - \pm y$. The third part with low excitation degree stays in the rapidity range from y_{\min} to $y_{\min} + \pm y$ and $y_{\max} - \pm y$ to y_{\max} .

For a given rapidity window, the P_T or m_T distribution of particles is contributed by the three parts in the thermalized cylinder. We can use the sum of three distributions described by Eq. (1) or (3) to give a fit for the experimental data. In the final state, the contributions of the three parts are the same if the concerned rapidity window is wide enough. For a narrow rapidity window, we treat the contributions of the three parts as free parameters in our calculation. Let γ_H , γ_M and γ_L denote the momentum distribution widths of particles produced in the three parts, respectively. The P_T and m_T distributions can be written as

$$f_{P_T}(P_T) = A_H f_{P_T}(P_T; \gamma_H) + A_M f_{P_T}(P_T; \gamma_M) + A_L f_{P_T}(P_T; \gamma_L); \quad (5)$$

and

$$f_{m_T}(m_T) = A_H f_{m_T}(m_T; \gamma_H) + A_M f_{m_T}(m_T; \gamma_M) + A_L f_{m_T}(m_T; \gamma_L); \quad (6)$$

respectively, where A_H , A_M and A_L denote the contributions of the three parts. In the calculation, the values of y_{\min} and y_{\max} do not need to be known because we treat the contributions of the three parts as free parameters.

III. Comparison with experimental data

Figure 1 presents the P_T distributions of negative hadrons (η^-) in two different rapidity windows, $y = 3.7 - 3.9$ (a) and $y = 4.7 - 4.9$ (b) in central Pb-Pb collisions at 158A GeV. The circles are the NA49 experimental data [22]. The curves are our calculated results using Eq. (5). In the calculation, we take $\gamma_H = 0.90$ GeV/c, $\gamma_M = 0.50$ GeV/c, and $\gamma_L = 0.22$ GeV/c for the different rapidity windows. The values of A_H , A_M , and A_L for Fig. 1(a) are 0.20, 0.44, and 0.36, and for Fig. 1(b) they are 0.10, 0.40, and 0.50, respectively. The calculated curve is scaled to the experimental data for a given rapidity window. The values of parameters are obtained by fitting the experimental data, and the method of χ^2 testing is used.

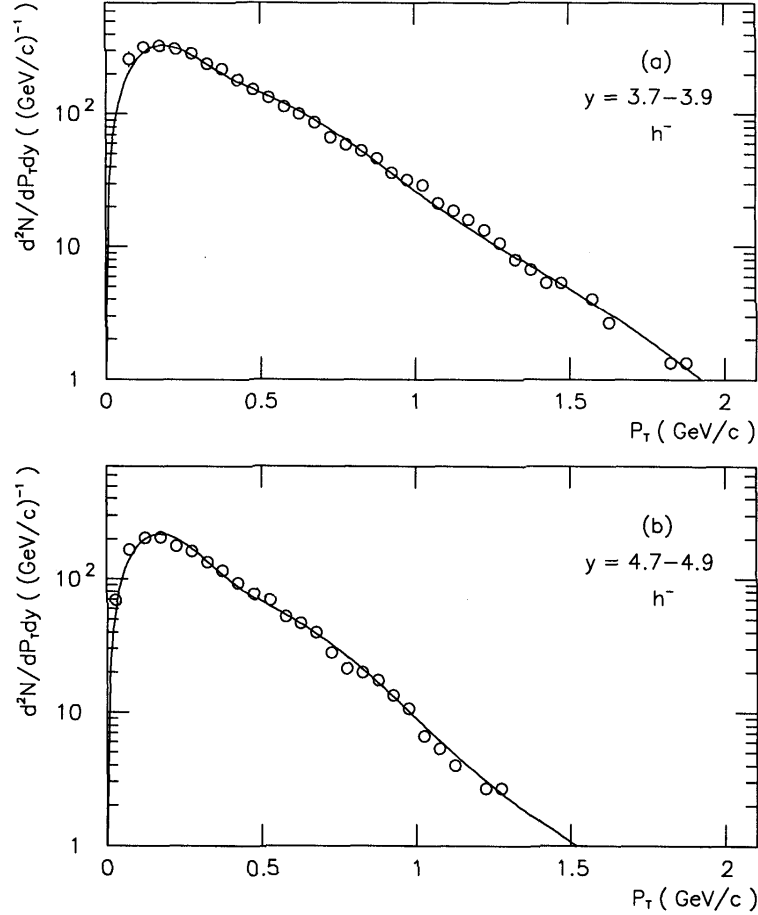


FIG. 1. Negative hadron P_T spectra in two different rapidity windows, $y = 3.7 ; 3.9$ (a) and $y = 4.7 ; 4.9$ (b), in central Pb-Pb collisions at 158A GeV. The circles are the experimental data of the NA49 Collaboration [22]. The curves are our calculated results.

Figure 2 is similar to Fig. 1, but it shows the m_T distributions of h^i in the rapidity windows $y = 3.7 ; 3.9$ (a) and $y = 4.7 ; 4.9$ (b) in central Pb-Pb collisions at 158A GeV. The circles are the NA49 experimental data [22]. The curves are our calculated results using Eq. (6). In the calculation, we have used the same parameter values as those for Fig. 1. All of the negative hadrons are treated as h^i . The calculated curve is scaled to the experimental data for a given rapidity window.

The values of A_H , A_M , and A_L for Figs. 1 and 2 reflect the contributions of the high excitation part, middle excitation part, and low excitation part in the concerned thermalized cylinder, respectively. In central Pb-Pb collisions at 158A GeV, we see that the middle excitation part has the most contribution in the rapidity window $y = 3.7 ; 3.9$, and the low excitation part has the

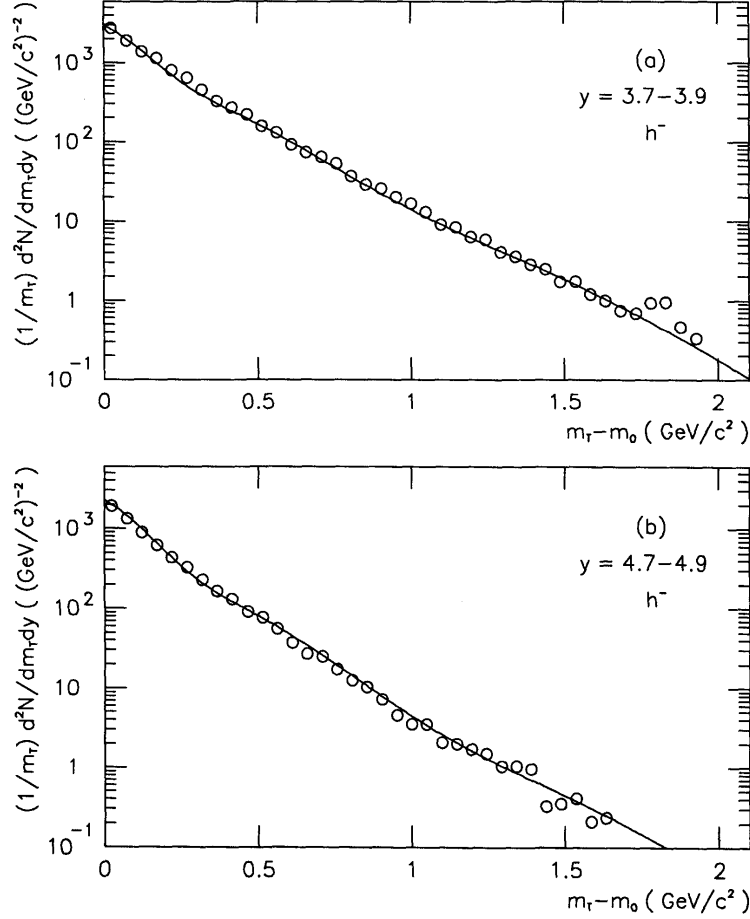


FIG. 2. As for Fig. 1, but showing the negative hadron m_T spectra.

most contribution in the rapidity window $y = 4.7 ; 4.9$. Our recent work [23] shows that $y_c = 2.91$, $y_{\min} = 1.21$, $y_{\max} = 4.61$, and $\pm y = 0.57$ for the concerned colliding system. In rapidity space, the high excitation part, middle excitation part, and low excitation part should be in $2.34 ; 3.48$, $1.78 ; 2.34$ and $3.48 ; 4.04$, and $1.21 ; 1.78$ and $4.04 ; 4.61$, respectively. We can see that the rapidity window $y = 3.7 ; 3.9$ is close to the middle excitation part, and the rapidity window $y = 4.7 ; 4.9$ is close to the low excitation part. This renders the middle excitation part as having the biggest contribution in the rapidity window $y = 3.7 ; 3.9$ and the low excitation part as having the biggest contribution in the rapidity window $y = 4.7 ; 4.9$.

The P_T distributions of net protons (p) in three different rapidity windows $y = 3.0 ; 3.2$ (a), $y = 4.0 ; 4.2$ (b), and $y = 5.0 ; 5.2$ (c) in central Pb-Pb collisions at 158A GeV are given in Fig. 3. The circles are the NA49 experimental data [22]. The curves are our calculated results using Eq. (5). In the calculation, we take $\frac{3}{4}H = 1.20 \text{ GeV/c}$, $\frac{3}{4}M = 0.90 \text{ GeV/c}$, and $\frac{3}{4}L = 0.60 \text{ GeV/c}$ for the different rapidity windows. The values of A_H , A_M , and A_L for Fig. 3(a) are 0.30,

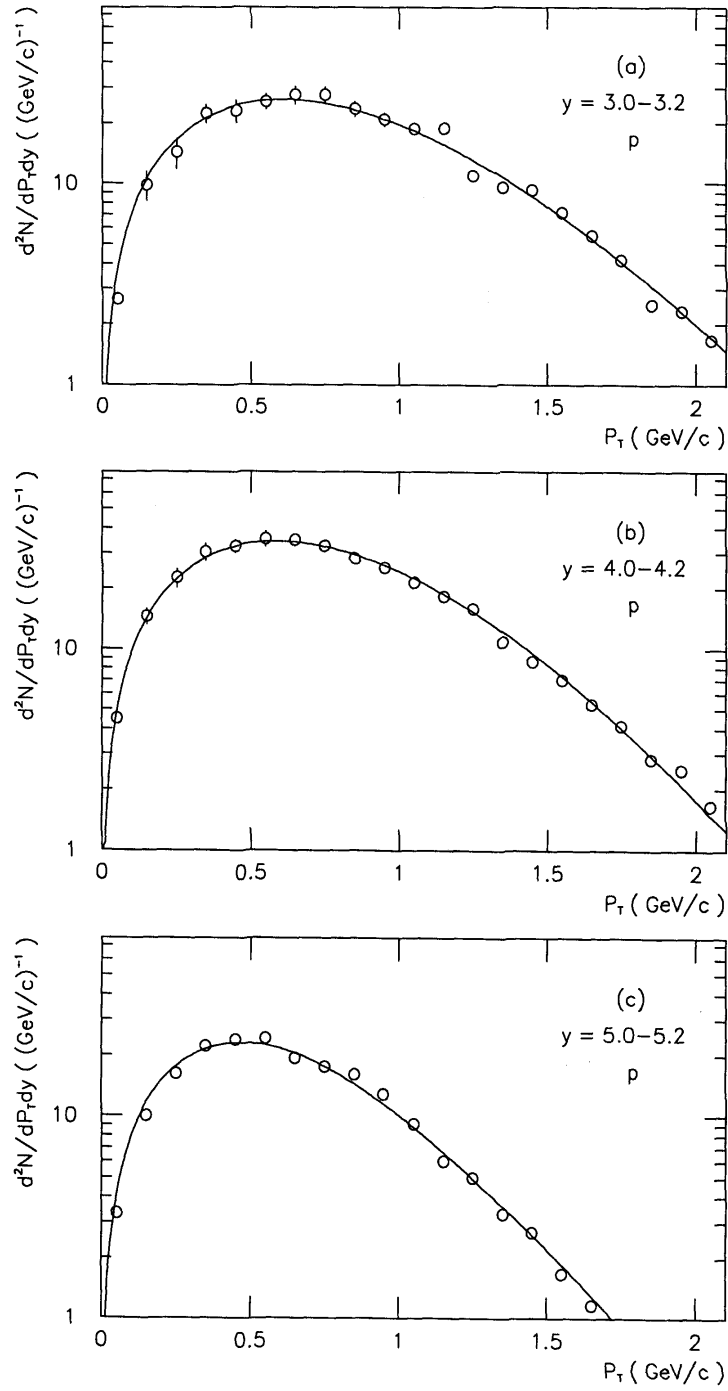


FIG. 3. Net proton P_T spectra in three different rapidity windows, $y = 3.0 ; 3.2$ (a), $y = 4.0 ; 4.2$ (b), and $y = 5.0 ; 5.2$, in central Pb-Pb collisions at 158A GeV. The circles are the experimental data of the NA49 Collaboration [22]. The curves are our calculated results.

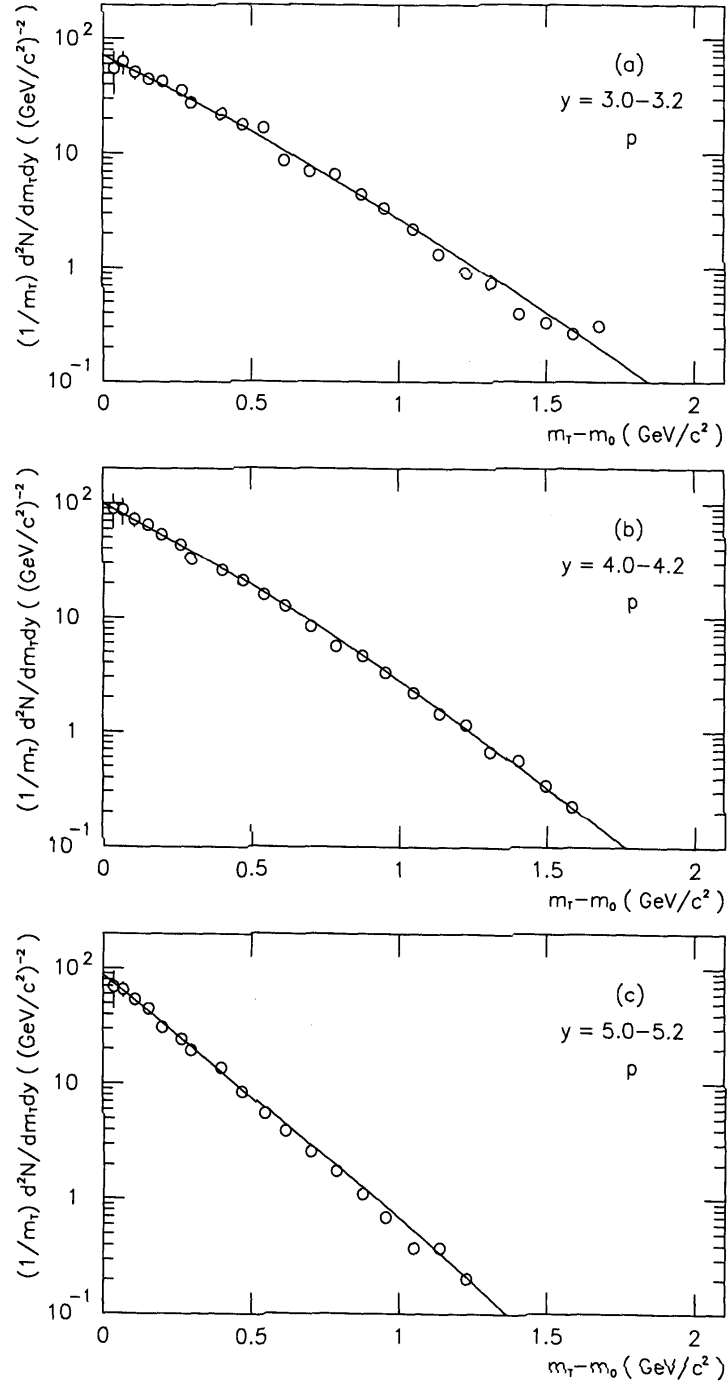


FIG. 4. As for Fig. 3, but showing the net proton m_T spectra.

0.60, and 0.10, for Fig. 3(b) they are 0.15, 0.72, and 0.13, and for Fig. 3(c) they are 0.00, 0.45, and 0.55, respectively. The calculated curve is scaled to the experimental data for a given rapidity window. The values of the parameters are obtained by fitting the experimental data, and the method of χ^2 testing is used.

Figure 4 is similar to Fig. 3, but it shows the m_T distributions of p in the rapidity windows $y = 3.0 ; 3.2$ (a), $y = 4.0 ; 4.2$ (b), and $y = 5.0 ; 5.2$ (c) in central Pb-Pb collisions at 158A GeV. The circles are the NA49 experimental data [22]. The curves are our calculated results using Eq. (6). In the calculation, we have used the same parameter values as those for Fig. 3. The calculated curve is scaled to the experimental data for a given rapidity window.

We can explain the significances of A_H , A_M , and A_L for Figs. 3 and 4 as compared to those for Figs. 1 and 2. The difference is that the values of y_{\min} , y_{\max} , and $\pm y$ for protons are different from those for negative hadrons. Meanwhile, the effect of leading protons has to be considered. The contribution of leading protons is in the low and high rapidity regions, i.e., the leading protons are in the low and middle excitation parts in the concerned thermalized cylinder. This renders the middle excitation part as having the biggest contribution in the rapidity windows $y = 3.0 ; 3.2$ and $y = 4.0 ; 4.2$ and the low excitation part as having the biggest contribution in the rapidity window $y = 5.0 ; 5.2$. Especially, the high excitation part has no contribution in the rapidity window $y = 5.0 ; 5.2$ because the part is so far from the window.

The momentum distribution width reflects the temperature of the emission source. Our results show that the momentum distribution width is bigger for protons than for negative hadrons. This indicates that the source temperature is greater for emitting protons than for emitting negative hadrons. We can say that the protons are emitted early and the negative hadrons are emitted late in the thermalized cylinder.

In the calculation of the P_T distribution, we do not need to consider m_0 . In the calculation of the m_T distribution, we treat all the negative hadrons as $\frac{1}{2}m_0$. If some of the negative hadrons were kaons or other particles, the value of m_0 should be changed. We have used the same parameter values for calculating both the P_T and m_T distributions. The corresponding results between the experimental data [22] and our calculation show that the contributions of kaons or other particles can be neglected in the investigation of the negative hadron m_T distribution in the concerned colliding system.

From Figs. 1-4 one can see that the multisource ideal gas model is successful in the descriptions of P_T and m_T distributions for h^{\pm} and p produced in central Pb-Pb collisions at 158A GeV. Our previous works [18-21] have studied the emissions of light nuclear fragments and relativistic particles. The two-source emission picture [18] and the thermalized cylinder model [19-21] can be contained in fact in the frame of the multisource ideal gas model.

IV. Conclusion

We have investigated the P_T and m_T distributions of negative hadrons and net protons produced in high-energy nucleus-nucleus collisions. Based on the multisource ideal gas model, the calculated results are in good agreement with the experimental data of the NA49 Collaboration. The transverse spectra show a multisource emission of produced particles. The hot and dense system formed in high-energy nucleus-nucleus collisions is estimated to be in local thermal equilibrium at the time of freeze-out.

Acknowledgements

This work was finished at the Cyclotron Institute of Texas A&M University and supported by the China Scholarship Council. The author's work was also supported by the Shanxi Provincial Foundation for Returned Overseas Scholars, Shanxi Provincial Foundation for Leading Specialists in Science, and Shanxi Provincial Science Foundation for Young Specialists.

References

E-mail: liufh@dns.sxtu.edu.cn

- [1] J. Geiss, W. Cassing and C. Greiner, Nucl. Phys. A **644**, 107 (1998).
- [2] S. A. Bass *et al.*, Prog. Part. Nucl. Phys. **41**, 225 (1998).
- [3] B. A. Li and C. M. Ko, Phys. Rev. C **52**, 2037 (1995).
- [4] H. Sorge, H. Stöcker and W. Greiner, Nucl. Phys. A **498**, 567c (1989).
- [5] K. Werner, Z. Phys. C **42**, 85 (1989).
- [6] A. Capella, U. Sukhatme, C. I. Tan and J. Tran Thanh Van, Phys. Rep. **236**, 225 (1994).
- [7] L. V. Bravina, N. S. Amelin, L. P. Csernai, P. Levai and D. Strottman, Nucl. Phys. A **544**, 461c (1994).
- [8] S. H. Kahana, D. E. Kahana, Y. Pang and T. J. Schlagel, Annu. Rev. Part. Sci. **46**, 31 (1996).
- [9] B. Anderson, G. Gustafson and H. Pi, Z. Phys. C **57**, 485 (1993); B. H. Sa and A. Tai, Comp. Phys. Commun. **90**, 121 (1995); B. H. Sa and A. Tai, Phys. Rev. C **55**, 2010 (1997); B. H. Sa and A. Tai, Phys. Rev. C **57**, 261 (1998); B. H. Sa and A. Tai, Phys. Lett. B **399**, 29 (1997); B. H. Sa and A. Tai, Phys. Lett. B **409**, 393 (1997).
- [10] W. Ehehalt and W. Cassing, Nucl. Phys. A **602**, 449 (1996).
- [11] A. Shor and R. Longacre, Phys. Lett. B **218**, 100 (1989).
- [12] X. N. Wang and M. Gyulassy, Phys. Rev. D **44**, 3501 (1991); X. N. Wang and M. Gyulassy, Phys. Rev. D **45**, 844 (1992).
- [13] K. Geiger, Phys. Rep. **258**, 237 (1995).
- [14] W. Y. Chang, Acta Phys. Sin. **17**, 271 (1961) (in Chinese) and references therein; G. D. Westfall *et al.*, Phys. Rev. Lett. **37**, 1202 (1976).
- [15] J. Letessier, J. Rafelski and A. Tounsi, Phys. Lett. B **292**, 417 (1992); J. Letessier *et al.*, Phys. Rev. D **51**, 3408 (1995).
- [16] C. Spieles, H. Stöcker and C. Greiner, Eur. Phys. J. C **2**, 351 (1998).
- [17] P. Braun-Munzinger, J. Stachel, J. P. Wessels and N. Xu, Phys. Lett. B **344**, 43 (1995); P. Braun-Munzinger, J. Stachel, J. P. Wessels and N. Xu, Phys. Lett. B **365**, 1 (1996).
- [18] F. H. Liu, Chin. J. Phys. **38**, 1063 (2000).
- [19] F. H. Liu and Y. A. Panebratsev, Nucl. Phys. A **641**, 379 (1998); F. H. Liu and Y. A. Panebratsev, Phys. Rev. C **59**, 1193 (1999); F. H. Liu and Y. A. Panebratsev, Phys. Rev. C **59**, 1798 (1999); F. H. Liu, Nuovo Cimento A **112**, 1167 (1999); F. H. Liu, Phys. Rev. D **62**, 074002 (2000). F. H. Liu, Phys. Rev. D **63**, 032001 (2001).
- [20] F. H. Liu, Can. J. Phys. **77**, 313 (1999); F. H. Liu, Can. J. Phys. **78**, 851 (2000).
- [21] F. H. Liu, Chin. J. Phys. **38**, 42 (2000); F. H. Liu, Chin. J. Phys. **38**, 907 (2000).
- [22] NA49 Collaboration, M. Y. Toy, Ph. D. thesis, University of California, Los Angeles, 1999.
- [23] F. H. Liu, Mod. Phys. Lett. A **15**, 1497 (2000).